

BEAMSPACE MIMO TRANSCEIVERS FOR LOW-COMPLEXITY AND NEAR-OPTIMAL COMMUNICATION AT MM-WAVE FREQUENCIES

Gi Hong Song John Brady Akbar Sayeed

Electrical & Computer Engineering
University of Wisconsin-Madison, Madison, WI 53706
Email: gsong4@wisc.edu, jhbrady@wisc.edu, akbar@engr.wisc.edu

ABSTRACT

Multiple-input multiple-output (MIMO) systems that exploit multi-antenna arrays and millimeter-wave systems operating in the 30-300GHz band offer synergistic opportunities for meeting the exploding data requirements of wireless networks. While combining these technologies offers the advantages of high-dimensional MIMO, it increases transceiver complexity dramatically in conventional MIMO approaches due to the large number of antennas required for optimal performance. On the other hand, the dimension of the communication subspace is typically much smaller than the system dimension in practice. By multiplexing data onto highly directional orthogonal beams, beamspace MIMO (B-MIMO) provides direct and near-optimum access to the low-dimensional communication subspace and dramatically lowers transceiver complexity when realized with analog beamforming. In this paper we present and analyze the capacity of several low-complexity B-MIMO transceivers for realizing multi-Gigabits/s speeds.

Index Terms— High-dimensional MIMO, Massive MIMO, Millimeter-wave communication, Beamforming, Gigabit wireless

1. INTRODUCTION

The capacity demands on wireless networks are growing exponentially with the proliferation of data intensive wireless devices, such as smart phones and tablets. In current wireless networks operating below 5 GHz, two main approaches are being pursued for addressing this challenge: the use of small cells to increase spatial re-use of spectrum [1], and the use of multi-antenna multiple-input multiple-output (MIMO) technology for managing interference and increasing spectral efficiency [2, 3]. Emerging millimeter-wave (mm-wave) systems, operating in the 30-300GHz range, offer a complementary, synergistic opportunity due to the orders-of-magnitude larger available bandwidth [4], as well as high-dimensional MIMO operation due to the small wavelengths [5, 6]. The large number of MIMO degrees of freedom can be exploited for a number of critical capabilities, including [4–7]: higher antenna/beamforming gain for enhanced power efficiency; higher spatial multiplexing gain for enhanced spectral efficiency; and highly directional communication with narrow beams for reduced interference and enhanced security.

Conventional MIMO approaches fall short of harnessing these opportunities at mm-wave frequencies: optimal operation requires a prohibitively high transceiver complexity due to the large number of antennas [4–6] and approaches to reducing complexity (e.g., antenna selection [8, 9] and widely spaced antennas [10–13]) are

sub-optimal and suffer from severe performance degradation [5, 6]. Due to the predominance of line-of-sight (LoS) and sparse multipath propagation at mm-wave frequencies [4, 14], the MIMO channels are expected to be severely low-rank: communication occurs in a low-dimensional subspace of the high-dimensional spatial signal space.

In this paper, we propose transceiver architectures that exploit the concept of beamspace MIMO (B-MIMO) communication – multiplexing data onto orthogonal spatial beams – for near-optimal performance at mm-wave frequencies with transceiver complexity that tracks the dimension of the communication subspace [5, 6]. Since the orthogonal beams serve as approximate channel eigenfunctions [5, 6, 15], the low channel rank is manifested in the sparsity of the beamspace channel matrix. This naturally leads to *beam selection* for near-optimum dimensionality reduction, which can be exploited for dramatic reduction in transceiver complexity on two fronts: digital signal processing (DSP) complexity as well as hardware complexity through the use of a hybrid analog-digital front-end that enables analog beamforming [5, 6, 16]. We develop and compare the capacity of three low-complexity linear B-MIMO transceivers for point-to-point links: the optimal singular-value-decomposition (SVD) transceiver, and the matched-filter (MF) and minimum-mean-squared-error (MMSE) transceivers that require channel state information only at the receiver [2, 3]. Our results show that the proposed B-MIMO transceivers can deliver multi-Gigabits/s (Gbps) speeds with practically viable complexity.

Related work: Currently mm-wave systems are used for commercial wireless backhaul systems that exploit the large antenna gains but no multiplexing gains, e.g. [17]. On the other hand, widely spaced MIMO systems (to reduce complexity) [10–13] have also been proposed that exploit multiplexing gain but suffer from reduced array gain and capacity [5, 6]. Analog beamforming via phase shifting networks in conventional antenna arrays has also been proposed for reducing mm-wave transceiver complexity [4, 18, 19]. Due to the small wavelengths, mm-wave B-MIMO transceivers are directly relevant to high-dimensional massive MIMO systems [7].

2. SYSTEM MODEL

This section develops the B-MIMO system model, including channel models for line of sight (LoS) and multipath propagation environments. For simplicity, we consider systems using 1D linear antennas – extension to 2D planar antennas is straightforward [5].

2.1. Sampled MIMO System Representation

Consider a linear antenna of length L . If the aperture is sampled with critical spacing, $d = \frac{\lambda}{2}$ where λ is the wavelength, there is no loss of information. The sampled points on the aperture are equivalent to a n -dimensional uniform linear array (ULA) of antennas, where $n = \lfloor \frac{2L}{\lambda} \rfloor$ is the maximum number of spatial modes supported by the

This work is partly supported by NSF under grants ECCS-1052628 and ECCS-1247583, and the Wisconsin Alumni Research Foundation.

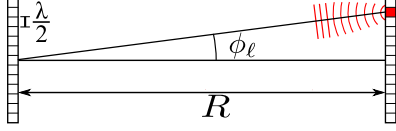


Fig. 1: Illustration of a LoS channel.

antenna/ULA and is proportional to its antenna/beamforming gain [5, 6, 15, 20]. Additionally, conventional MIMO approaches require n antenna elements for optimal performance. A MIMO system with ULAs at the transmitter and the receiver can be modeled as

$$\mathbf{r} = \mathbf{H}\mathbf{x} + \mathbf{w} \quad (1)$$

where \mathbf{H} is the $n_R \times n_T$ aperture domain channel matrix representing coupling between the transmitter and receiver ULA elements, \mathbf{x} is the n_T -dimensional transmitted signal vector, \mathbf{r} is the n_R -dimensional received signal vector, and $\mathbf{w} \sim \mathcal{CN}(\mathbf{0}, \mathbf{I})$ is the n_R -dimensional vector of unit variance additive white Gaussian noise.

2.2. Beamspace MIMO System Representation

The B-MIMO system representation is obtained from (1) via fixed beamforming at the transmitter and the receiver. Each column of the beamforming matrix, \mathbf{U}_n , is an array steering/response vector at a specified angle [5, 6, 15]. For a critically spaced ULA, a plane wave in the direction of angle ϕ (see Fig. 1) corresponds to a spatial frequency, $\theta = 0.5 \sin(\phi)$, and the corresponding array steering/response (column) vector is given by [15]

$$\mathbf{a}_n(\theta) = [\exp(-j2\pi\theta i)]_{i \in \mathcal{I}(n)} \quad (2)$$

where $\mathcal{I}(n) = \{i - (n-1)/2 : i = 0, \dots, n-1\}$ is a symmetric set of indices for a given n . The columns of \mathbf{U}_n correspond to n fixed spatial frequencies/angles with uniform spacing $\Delta\theta_o = \frac{1}{n}$:

$$\mathbf{U}_n = \frac{1}{\sqrt{n}} [\mathbf{a}_n(\Delta\theta_o i)]_{i \in \mathcal{I}(n)} \quad (3)$$

which represent n orthogonal beams, with beamwidth $\Delta\theta_o$, that cover the entire spatial horizon ($-\pi/2 \leq \phi \leq \pi/2$) and form a basis for the n -dimensional spatial signal [15]. In fact, \mathbf{U}_n is a unitary discrete Fourier transform (DFT) matrix: $\mathbf{U}_n^H \mathbf{U}_n = \mathbf{U}_n \mathbf{U}_n^H = \mathbf{I}$. The overall beamspace system representation is obtained from (1) as

$$\mathbf{r}_b = \mathbf{H}_b \mathbf{x}_b + \mathbf{w}_b, \quad \mathbf{H}_b = \mathbf{U}_{n_R}^H \mathbf{H} \mathbf{U}_{n_T} \quad (4)$$

where $\mathbf{x}_b = \mathbf{U}_{n_T}^H \mathbf{x}$, $\mathbf{r}_b = \mathbf{U}_{n_R}^H \mathbf{r}$, and $\mathbf{w}_b = \mathbf{U}_{n_R}^H \mathbf{w}$ are the transmitted, received, and noise signal vectors in beamspace. Since \mathbf{U}_{n_T} and \mathbf{U}_{n_R} are unitary DFT matrices, \mathbf{H}_b is a 2D DFT of \mathbf{H} and thus a completely equivalent representation of \mathbf{H} [5, 15].

2.3. Channel Modeling

Due to the highly directional nature of propagation at mm-wave, LoS propagation is expected to be the dominant mode, with some additional sparse (single-bounce) multipath components possible in urban environments [4, 14]. For LoS channels, \mathbf{H} is deterministic and can be accurately approximated in terms of array response vectors [5, 6]. As illustrated in Fig. 1, the n_T columns of \mathbf{H} can be constructed via array response vectors corresponding to the spatial frequencies induced by the different transmitter ULA elements [5, 6]:

$$\mathbf{H} = [\mathbf{a}_{n_R}(\theta_\ell)]_{\ell \in \mathcal{I}(n_T)}, \quad \theta_\ell = \Delta\theta_{ch}\ell \approx \frac{\lambda}{4R}\ell. \quad (5)$$

The rank of the LoS channel matrix, p_{los} , is typically much smaller than n_R , n_T if the link length R is large compared to the antenna

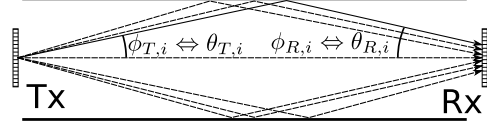


Fig. 2: Illustration of a single-bounce sparse multipath channel.

dimensions L_T and L_R . Given the above construction of \mathbf{H} in terms of array vectors, the rank can be accurately estimated by the number of orthogonal transmit beams that span the receiver aperture [5, 6]: $p_{los} \approx \frac{2\Delta\theta_{max,R}}{\Delta\theta_{o,T}} + 1 \approx \frac{L_T L_R}{R\lambda} + 1$, where $\Delta\theta_{max,R}$ is the range of spatial frequencies induced by the receiver array at the transmitter. Furthermore, orthogonal steering vectors serve as approximate eigenfunctions of \mathbf{H} : only an approximately $p_{los} \times p_{los}$ sub-matrix of \mathbf{H}_b is non-zero and approximately diagonal (see Fig. 4a).

A stochastic multipath channel can be modeled as [15]

$$\mathbf{H} = \sum_{i=0}^{N_p} \beta_i \mathbf{a}_{n_R}(\theta_{R,i}) \mathbf{a}_{n_T}^H(\theta_{T,i}) \quad (6)$$

where N_p denotes the number of paths and β_i , $\theta_{R,i}$ and $\theta_{T,i}$ represent the complex amplitude, angle of arrival (AoA), and angle of departure (AoD) of the i^{th} path. The $i = 0$ path is the LoS path with $\beta_0 = 1$ and $\theta_{T,0} = \theta_{R,0} = 0$. For the other paths, β_i can be modeled as $\beta_i = |\beta_i| \exp(-j\psi_i)$ where $|\beta_i|^2$ represents path loss (between -5 and -10dB for single-bounce paths with higher attenuation for multi-bounce paths [14]), and ψ_i is uniformly distributed in $[0, 2\pi]$. Fig. 2 shows a simple physical model of a sparse multipath channel: buildings alongside the road create single-bounce multipath propagation. We assume that the link length R is large enough so that $|\theta_{R,i}| \in [\Delta\theta_{o,R} - \frac{\Delta\theta_{o,R}}{4}, \Delta\theta_{o,R} + \frac{\Delta\theta_{o,R}}{4}]$ and $|\theta_{T,i}| \in [\Delta\theta_{o,T} - \frac{\Delta\theta_{o,T}}{4}, \Delta\theta_{o,T} + \frac{\Delta\theta_{o,T}}{4}]$, where $\Delta\theta_{o,T} = 1/n_T$, $\Delta\theta_{o,R} = 1/n_R$, and $\text{sign}(\theta_{R,i}) = \text{sign}(\theta_{T,i})$. This leads to $p_{mp} = 3$ orthogonal beams coupling the transmitter and the receiver, resulting in an \mathbf{H} with approximate rank $p_{mp} = 3$; \mathbf{H}_b only has a $p_{mp} \times p_{mp}$ non-zero sub-matrix that is nearly diagonal (see Fig. 4d).

3. LOW-DIMENSIONAL BEAMSPACE TRANSCEIVERS

We now outline a framework for B-MIMO transceiver design for achieving near-optimal performance with complexity comparable to the low dimension of the communication subspace.

3.1. Low-Dimensional B-MIMO Channel

Let $\sigma_c^2 = \text{tr}(\mathbf{H}_b^H \mathbf{H}_b) = \text{tr}(\mathbf{H}^H \mathbf{H}) = n_T n_R$ denote the LoS channel power. The low-dimensional communication subspace is captured by the SVD of \mathbf{H} : $\mathbf{H} = \mathbf{U}\mathbf{\Lambda}\mathbf{V}^H$, where $\mathbf{\Lambda}$ is a diagonal matrix of (ordered) singular values: $\lambda_1 \geq \lambda_2 \dots \lambda_{n_o}$ where $n_o = \min(n_T, n_R)$. In particular, most of the channel power is captured by p_{los} dominant singular values. We define the effective channel rank, $p_{eff} \approx p_{los}$, as the number of singular values that capture most of channel power: $\sum_{i=1}^{p_{eff}} \lambda_i^2 \geq \eta \sigma_c^2$, for some η close to 1 (e.g., 0.95). Optimal communication over the p_{eff} -dimensional communication subspace is achieved through the corresponding right and left singular vectors in \mathbf{V} and \mathbf{U} [5, 6].

In B-MIMO, the low-dimensional communication subspace is accessed through Fourier basis vectors, i.e. the columns of \mathbf{U}_{n_T} and \mathbf{U}_{n_R} in (4), that serve as approximate channel singular vectors [5, 15]. The channel power is concentrated in a low-dimensional sub-matrix, $\tilde{\mathbf{H}}_b$, of \mathbf{H}_b whose entries capture most of the channel power. Let $\Sigma_{T,b} = \mathbf{H}_b^H \tilde{\mathbf{H}}_b$ and $\Sigma_{R,b} = \tilde{\mathbf{H}}_b \mathbf{H}_b^H$ denote the transmit and

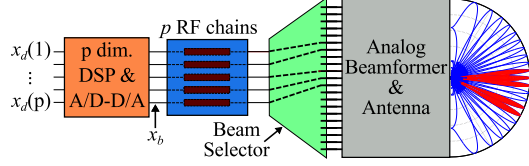


Fig. 3: A B-MIMO transceiver with analog beamforming.

receive beamspace correlation matrices. We define $\tilde{\mathbf{H}}_b$ as

$$\tilde{\mathbf{H}}_b = [H_b(i, j)]_{i \in \mathcal{M}_R, j \in \mathcal{M}_T} \quad (7)$$

where $\mathcal{M}_T = \{i : \Sigma_{T,b}(i, i) > \gamma_T \max_i \Sigma_{T,b}(i, i)\}$ and \mathcal{M}_R is defined similarly. The thresholds γ_T and γ_R are chosen so that

$$\sum_{i \in \mathcal{M}_T} \Sigma_{T,b}(i, i) \approx \sum_{i \in \mathcal{M}_R} \Sigma_{R,b}(i, i) \geq \eta_b \sigma_c^2, \quad (8)$$

with $\eta_b \approx \eta$ so that $\tilde{\mathbf{H}}_b$ captures the low-dimensional communication subspace. Finally, define $p_{eff,T} = |\mathcal{M}_T|$, $p_{eff,R} = |\mathcal{M}_R|$ and $p_{eff,b} = \min(p_{eff,T}, p_{eff,R})$, which is the number of beamspace modes. As we will see, $p_{eff,b} \approx p_{eff}$ and because of (8) the resulting performance is near-optimum. The above discussion applies to deterministic LoS channels. For stochastic multipath channels, \mathcal{M}_T and \mathcal{M}_R in (7) are determined using *statistical* channel covariance matrices, $\Sigma_{T,b} = E[\mathbf{H}_b^H \mathbf{H}_b]$ and $\Sigma_{R,b} = E[\mathbf{H}_b \mathbf{H}_b^H]$ with channel power $\sigma_c^2 = \text{tr}(\Sigma_{T,b}) = \text{tr}(\Sigma_{R,b}) = n_T n_R \sum_{i=0}^{N_p} E[|\beta_i|^2]$.

3.2. Optimal Transceiver Architecture

The performance benchmark is provided by the SVD transceiver in which independent data streams are communicated over channel singular vectors to eliminate interference. The transmitted signal in (1) is precoded as $\mathbf{x} = \mathbf{V} \mathbf{x}_e$ and the received signal is transformed as $\mathbf{r}_e = \mathbf{U}^H \mathbf{r}$ to result in non-interfering eigen channels: $\mathbf{r}_e = \Lambda \mathbf{x}_e + \mathbf{w}_e$, where $\mathbf{w}_e \sim \mathcal{CN}(\mathbf{0}, \mathbf{I})$. The capacity-achieving transmitted signal \mathbf{x}_e consists of independent Gaussian signals: $\mathbf{x}_e \sim \mathcal{CN}(\mathbf{0}, \Lambda_s)$ with $\Lambda_s = \text{diag}(\rho_1, \dots, \rho_{n_o})$ representing the allocation of total transmit power ρ over different channels, $\rho = E[\|\mathbf{x}\|^2] = \sum_i \rho_i$. For a given channel realization, the conditional capacity is

$$C(\rho|\mathbf{H}) = \max_{\rho_i: \sum_i \rho_i = \rho} \sum_{i=1}^{n_o} \log(1 + \text{SNR}_i(\mathbf{H})), \quad (9)$$

which represents the optimal power allocation via water-filling [21], with the signal-to-noise-ratio (SNR) for the i^{th} channel given by $\text{SNR}_i(\mathbf{H}) = \rho_i \lambda_i^2$. Power will be mainly allocated to the p_{eff} dominant channels. For deterministic LoS channels, i.e. \mathbf{H} is fixed, (9) represents the capacity: $C(\rho) = C(\rho|\mathbf{H})$. For stochastic multipath channels, the ergodic capacity is obtained by averaging over the channel statistics: $C(\rho) = E[C(\rho|\mathbf{H})]$.

The low-dimensional B-MIMO transceivers operate on the $p_{eff,R} \times p_{eff,T}$ sub-system of (4) induced by $\tilde{\mathbf{H}}_b$: $\tilde{\mathbf{r}}_b = \tilde{\mathbf{H}}_b \tilde{\mathbf{x}}_b + \tilde{\mathbf{w}}_b$. We focus on the class of linear transceivers which use a precoding matrix \mathbf{G} at the transmitter ($\tilde{\mathbf{x}}_b = \mathbf{G} \mathbf{x}_d$) and a filter matrix \mathbf{F} at the receiver ($\mathbf{r}_d = \mathbf{F}^H \tilde{\mathbf{r}}_b$) to yield the following system equation

$$\mathbf{r}_d = \mathbf{F}^H \tilde{\mathbf{H}}_b \mathbf{G} \mathbf{x}_d + \mathbf{w}_d. \quad (10)$$

The optimal low-dimensional transceiver is now determined by the SVD of $\tilde{\mathbf{H}}_b$, $\tilde{\mathbf{H}}_b = \tilde{\mathbf{U}} \tilde{\Lambda} \tilde{\mathbf{V}}^H$, and choosing $\mathbf{G} = \tilde{\mathbf{V}}$ and $\mathbf{F} = \tilde{\mathbf{U}}$ to create $p_{eff,b} \approx p_{eff}$ non-interfering channels. The optimal transmitted signal \mathbf{x}_d is again an independent Gaussian vector and, for a

given $\tilde{\mathbf{H}}_b$, the system capacity is

$$C(\rho|\tilde{\mathbf{H}}_b) = \max_{\rho_i: \sum_i \rho_i = \rho} \sum_{i=1}^{p_{eff,b}} \log(1 + \text{SNR}_i(\tilde{\mathbf{H}}_b)), \quad (11)$$

with $\text{SNR}_i(\tilde{\mathbf{H}}_b) = \rho_i \tilde{\lambda}_i^2$, where the $\tilde{\lambda}_i$ are the ordered singular values of $\tilde{\mathbf{H}}_b$, and the ergodic capacity is $C(\rho) = E[C(\rho|\tilde{\mathbf{H}}_b)]$.

3.3. Sub-optimal Beamspace Transceivers

The optimal SVD transceivers require channel state information (CSI), i.e. knowledge of \mathbf{H} or $\tilde{\mathbf{H}}_b$, at both the transmitter and the receiver, which is impractical in many situations. Thus, we consider two sub-optimal but simple B-MIMO transceivers for $\tilde{\mathbf{H}}_b$ that require CSI ($\tilde{\mathbf{H}}_b$) only at the receiver. For the sub-optimal transceivers we assume that $p_{eff,b} = p_{eff,T} \leq p_{eff,R}$. In both transceivers $\mathbf{G} = \mathbf{I}$ and the transmitted signal \mathbf{x}_d in (10) is an independent Gaussian vector with equal power allocation over the $p_{eff,b}$ beams: $\mathbf{x}_d \sim \mathcal{CN}(\mathbf{0}, \rho \mathbf{I}/p_{eff,b})$. The transceivers differ in their choice of \mathbf{F} for suppressing interference at the receiver. In the matched filter (MF) transceiver, $\tilde{\mathbf{F}}_{MF} = \tilde{\mathbf{H}}_b$, and (10) becomes $\mathbf{r}_d = \tilde{\mathbf{H}}_b^H \tilde{\mathbf{H}}_b \mathbf{x}_d + \mathbf{w}_d$. Since $\tilde{\mathbf{H}}_b^H \tilde{\mathbf{H}}_b$ is diagonally dominant, the interference is limited but still present. In the Minimum Mean Squared Error (MMSE) transceiver [22], \mathbf{F} is chosen to minimize the MSE at the receiver to further suppress interference, $\tilde{\mathbf{F}}_{MMSE} = \arg \min_{\mathbf{F}} E[\|\mathbf{F}^H \tilde{\mathbf{r}}_b - \mathbf{x}_d\|^2]$:

$$\tilde{\mathbf{F}}_{MMSE}^H = \mathbf{Q} \tilde{\mathbf{H}}_b^H (\tilde{\mathbf{H}}_b \mathbf{Q} \tilde{\mathbf{H}}_b^H + \mathbf{I})^{-1} \quad (12)$$

where $\mathbf{Q} = E[\mathbf{x}_d \mathbf{x}_d^H]$ is the covariance matrix of \mathbf{x}_d which equals $\mathbf{Q} = \frac{\rho}{p_{eff,b}} \mathbf{I}$ under independent and equal-power signaling. For both sub-optimal transceivers, the conditional capacity is

$$C(\rho|\tilde{\mathbf{H}}_b) = \sum_{i=1}^{p_{eff,b}} \log(1 + \text{SINR}_i(\tilde{\mathbf{H}}_b)) \quad (13)$$

where the interference is treated as noise and the signal-to-interference-and-noise-ratio (SINR) for the i^{th} data stream is

$$\text{SINR}_i(\tilde{\mathbf{H}}_b) = \frac{|\mathbf{f}_i^H \tilde{\mathbf{H}}_b \mathbf{g}_i|^2 \rho_i}{\sum_{j \neq i} |\mathbf{f}_i^H \tilde{\mathbf{H}}_b \mathbf{g}_j|^2 \rho_j + \|\mathbf{f}_i\|^2}, \quad (14)$$

and $\rho_i = \rho/p_{eff,b}$. For stochastic channels, the ergodic capacity is $C(\rho) = E[C(\rho|\tilde{\mathbf{H}}_b)]$.

Transceiver Complexity: B-MIMO communication can be achieved in conventional MIMO transceivers by accessing the $p_{eff,T}$ transmit beams in \mathcal{M}_T and $p_{eff,R}$ receive beams in \mathcal{M}_R through *digital beamforming* (via \mathbf{U}_{n_T} or \mathbf{U}_{n_R}) to reduce the DSP complexity from $\mathcal{O}(n)$ to $\mathcal{O}(p_{eff})$. However, the transceiver still requires n radio frequency (RF) chains to drive each antenna in the n -dimensional ULA. Conversely, as shown in Fig. 3, B-MIMO transceivers realized with *analog beamforming* (e.g. through a discrete lens array [5, 6, 16]) additionally reduce the hardware complexity from n to $\mathcal{O}(p_{eff})$ by only allocating RF chains directly to the $p_{eff,T}$ or $p_{eff,R}$ selected beams. This reduction in hardware complexity is critical, due to the large values of n (1000-10000) at mm-wave frequencies [5, 6].

4. NUMERICAL RESULTS

We now present numerical capacity results for B-MIMO transceivers at $f_c = 80\text{GHz}$ for both LoS and multipath channels, with results at

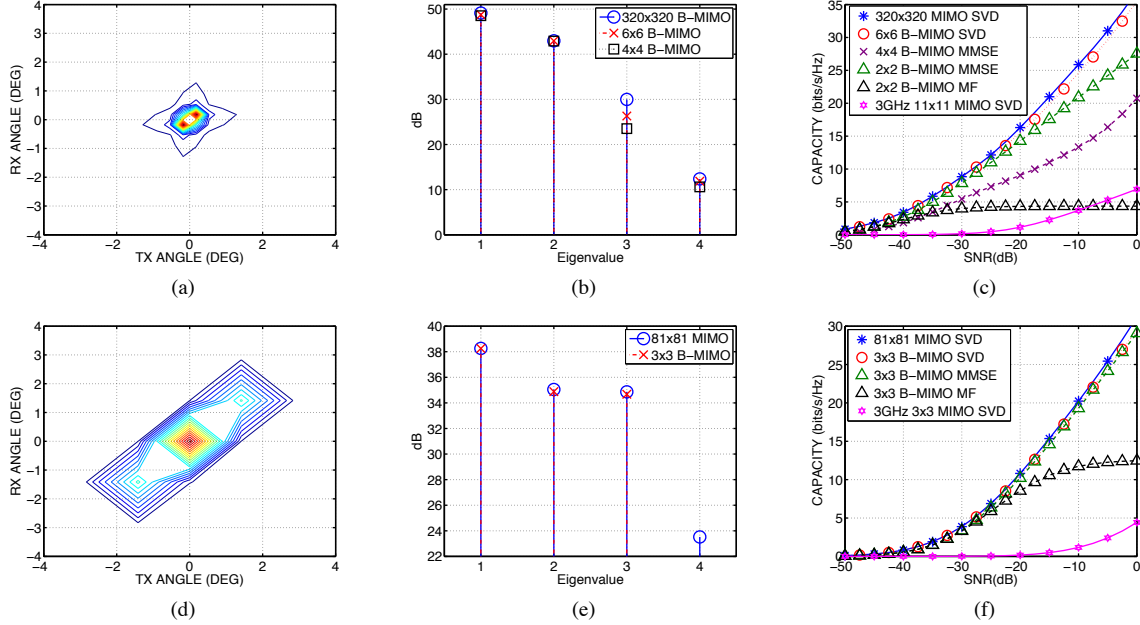


Fig. 4: (a)-(c): LoS channel: (a) Contour plot of $|\mathbf{H}_b|^2$ with $n = 320$ and $p_{los} = 2$, (b) 4 largest eigenvalues of $\tilde{\mathbf{H}}_b^H \tilde{\mathbf{H}}_b$ and $\mathbf{H}^H \mathbf{H}$ in dB scale, and (c) Capacity of different transceivers. (d)-(f): Multipath channel: (d) Contour plot of $E[|\mathbf{H}_b|^2]$ with $n = 81$ and $p_{mp} = 3$; (e) 4 largest eigenvalues of $E[\tilde{\mathbf{H}}_b^H \tilde{\mathbf{H}}_b]$ and $E[\mathbf{H}^H \mathbf{H}]$ in dB scale, and (f) Capacity of different transceivers.

$f_c = 3\text{GHz}$ using the optimal SVD transceiver included for comparison. The absolute SNR values considered are not critical, the relative performance of the different transceivers at a particular SNR is what matters. Calibration to operational SNR values can be achieved through normalization of the channel power [16].

Fig. 4a shows a contour plot of $|\mathbf{H}_b|^2$ for a LoS channel with $L_T = L_R = 0.60\text{m}$ and $R = 100\text{m}$ which yields $n_T = n_R = 320$ and $p_{los} = 2$ at 80GHz . Using $p_{eff} = 4$ singular values of \mathbf{H} yields $\eta \approx 1$. Using $\gamma_T = \gamma_R = 0.02$ results in a $6 \times 6 \tilde{\mathbf{H}}_b$ ($p_{eff,b} = 6$) that captures 93% of the channel power ($\eta_b = 0.93$) vs 89% when $p_{eff,b} = 4$. As shown in Fig. 4b, this allows $\tilde{\mathbf{H}}_b$ to better capture the dominant eigenvalues of \mathbf{H} . Fig. 4c shows the capacity of the different transceivers for the LoS channel. The capacity of the low-dimensional 6×6 B-MIMO SVD system corresponding to $\tilde{\mathbf{H}}_b$ is nearly identical to that of 320×320 SVD system corresponding to \mathbf{H} . The 2×2 B-MIMO MMSE transceiver closely approximates the performance of the SVD transceiver until an SNR of about -20dB (when it begins allocating power to the 3rd mode). On the other hand, because it allocates equal power to all beamspace modes, the 4×4 B-MIMO MMSE transceiver suffers from performance degradation. The MMSE transceivers effectively suppress interference, which is not negligible as evident from the performance degradation in the MF transceiver at higher SNRs. At 3GHz , the channel yields $n_T = n_R = 11$ and $p_{los} = 1$, and substantially lower capacity.

Fig. 4d shows contour plot of $E[|\mathbf{H}_b|^2]$ for a multipath channel with $L_T = L_R = 0.15\text{m}$ and $R = 200\text{m}$, yielding $n_T = n_R = 81$ at 80GHz . While only a single LoS mode can be exploited at 80GHz ($p_{los} = 1$), there are $N_p = 10$ additional single-bounce paths with $|\beta_i|^2 = -10\text{dB}$ (see Fig. 2) yielding $p_{mp} = 3$ as discussed in Sec. 2.3. Using 3 dominant eigenvalues of $E[\mathbf{H}^H \mathbf{H}]$ values results in $\eta = 0.98$. Using $\gamma_T = \gamma_R = 0.05$ yields a $3 \times 3 \tilde{\mathbf{H}}_b$. As shown in Fig. 4e, the eigenvalues of $E[\tilde{\mathbf{H}}_b^H \tilde{\mathbf{H}}_b]$ are nearly identical to the eigenvalues of $E[\mathbf{H}^H \mathbf{H}]$ and capture 96% of the channel power ($\eta_b = 0.96$). Again, despite the dimensionality reduc-

tion from $n = 81$ to $p = 3$, the capacities of the reduced and full dimensional SVD systems are nearly identical. The 3×3 B-MIMO MMSE transceiver closely approximates the performance of the 3×3 B-MIMO SVD transceiver and again the MF transceiver's performance degrades at higher SNRs. The multipath channel results were obtained by averaging over 1000 channel realizations. At 3GHz , $n_T = n_R = 3$ and we assume the most favorable setting of independent and identically distributed (Rayleigh) channel entries [3] and the same channel power as at 80GHz .

At an SNR of -20dB the low-complexity B-MIMO MMSE transceivers have capacities of 14.3 bits/s/Hz in the LoS channel and 10.2 bits/s/Hz in the multipath channel vs 1.1 bits/s/Hz and 0.17 bits/s/Hz for the 3GHz SVD transceivers. Using 10% fractional bandwidth (8GHz or 300MHz) the B-MIMO MMSE transceivers can achieve data rates of 114 Gbps in the LoS channel and 81.6 Gbps in the multipath channel, while the 3GHz SVD transceivers can achieve data rates of 330 Mbps and 51 Mbps respectively. When equipped with analog beamforming front ends, B-MIMO transceivers can achieve these multi-Gbps speeds with dramatically lower transceiver complexity compared to conventional MIMO.

5. CONCLUSION

We have presented low-complexity B-MIMO transceivers that deliver near-optimal performance in high-dimensional MIMO systems at mm-wave and higher frequencies. For both LoS and sparse-multipath channels, we first demonstrated that thresholding-based beam selection enables near-optimal access to the low-dimensional communication subspace of the high-dimensional MIMO channel. Secondly, we showed that the performance of the low-complexity MMSE transceiver closely approximates the performance of the optimal SVD transceiver in beamspace. In conjunction with analog beamforming front-ends [5,6,16], B-MIMO transceivers can achieve near-optimal performance with dramatically lower transceiver complexity compared to conventional MIMO approaches, providing a practical route for realizing the full potential of mm-wave MIMO.

6. REFERENCES

- [1] V. Chandrasekhar, J. Andrews, and A. Gatherer, "Femtocell networks: A survey," *IEEE Comm. Mag.*, vol. 331, no. 6018, pp. 717–719, Sept 2007.
- [2] A. Goldsmith, *Wireless Communications*, Cambridge University Press, Cambridge, MA, 2006.
- [3] I. E. Telatar, "Capacity of Multi-antenna Gaussian Channels," *European Transactions on Telecommunications*, vol. 10, no. 6, pp. 585–595, 1999.
- [4] Z. Pi and F. Khan, "An Introduction to Millimeter-Wave Mobile Broadband Systems," *IEEE Comm. Mag.*, vol. 49, no. 6, pp. 101–107, June 2011.
- [5] A. M. Sayeed and N. Behdad, "Continuous Aperture Phased MIMO: Basic Theory and Applications," in *Proc. Allerton Conference*, Sept. 29-Oct. 1 2010, pp. 1196–1203.
- [6] A. M. Sayeed and N. Behdad, "Continuous Aperture Phased MIMO: A new architecture for optimum line-of-sight links," in *Antennas and Propagation (APSURSI), 2011 IEEE International Symposium on*, July 2011, pp. 293–296.
- [7] T. L. Marzetta, "Noncooperative Cellular Wireless with Unlimited Numbers of Base Station Antennas," *IEEE Trans. Wireless Comm.*, vol. 9, no. 11, pp. 3590–3600, Nov. 2010.
- [8] S. Sanayei and A. Nosratinia, "Antenna selection in MIMO systems," *IEEE Comm. Mag.*, vol. 42, no. 10, pp. 68–73, Oct. 2004.
- [9] A. Mohammadi and F. Ghannouchi, "Single RF front-end MIMO transceivers," *IEEE Comm. Mag.*, vol. 49, no. 12, pp. 104–109, Dec. 2011.
- [10] E. Torkildson, B. Ananthasubramaniam, U. Madhow, and M. Rodwell, "Millimeter-wave MIMO: Wireless links at optical speeds," in *Proc. Allerton Conference*, Sept. 2006.
- [11] C. Sheldon, M. Seo, E. Torkildson, M. Rodwell, and U. Madhow, "Four-channel spatial multiplexing over a millimeter-wave line-of-sight link," in *Proc. 2011 IEEE MTT-S Int. Microwave Symp.*, June 2009, pp. 389–392.
- [12] F. Bohagen, P. Orten, and G. Oien, "Design of optimal high-rank line-of-sight MIMO channels," *IEEE Trans. Wireless Comm.*, vol. 6, no. 4, pp. 1420–1425, Apr. 2007.
- [13] I. Sarris and R. Nix, "Maximum MIMO capacity in line-of-sight," in *2005 International Conference on Information, Communications, and Signal Processing*, 2005, pp. 1236–1240.
- [14] T. S. Rappaport, E. Ben-Dor, J. N. Murdock, and Y. Qiao, "38 GHz and 60 GHz Angle-dependent Propagation for Cellular & Peer-to-Peer Wireless Communications," in *IEEE International Conference on Communications (ICC)*, June 2012.
- [15] A. M. Sayeed, "Deconstructing Multiantenna Fading Channels," *IEEE Trans. Signal Processing*, vol. 50, no. 10, pp. 2563–2579, Oct. 2002.
- [16] J. Brady, N. Behdad, and A. M. Sayeed, "Beamspace MIMO for Millimeter-Wave Communications: System Architecture, Modeling, Analysis, and Measurements," *IEEE Trans. Antennas and Propagation* to be published.
- [17] "Flexport μ Wave: A Better Approach to High-Capacity Microwave Backhaul," BridgeWave Communications White Paper, 2011.
- [18] V. Venkateswaran and A. van der Veen, "Analog Beamforming in MIMO Communications With Phase Shift Networks and Online Channel Estimation," *IEEE Trans. Signal Processing*, vol. 58, no. 8, pp. 4131–4143, Aug. 2010.
- [19] O. El Ayach, R.W. Heath, S. Abu-Surra, S. Rajagopal, and Zhouyue Pi, "The Capacity Optimality of Beam Steering in Large Millimeter Wave MIMO Systems," in *Signal Processing Advances in Wireless Communications (SPAWC), 2012 IEEE 13th International Workshop on*, June 2012, pp. 100–104.
- [20] R. J. Mailloux, *Phased Array Antenna Handbook*, Artech House, 2nd edition, 2005.
- [21] T. M. Cover, *Elements of Information Theory*, Wiley, New York, 1991.
- [22] S. M. Kay, *Fundamentals of Statistical Signal Processing*, Prentice Hall, Englewood Cliffs, N.J., 1993.